Articles

Synthesis, Stability, Antiviral Activity, and Protease-Bound Structures of Substrate-Mimicking Constrained Macrocyclic Inhibitors of HIV-1 Protease

Joel D. A. Tyndall,[†] Robert C. Reid,[†] David P. Tyssen,[§] Darren K. Jardine,[§] Belinda Todd,[‡] Margaret Passmore,[†] Darren R. March,[†] Leonard K. Pattenden,[†] Douglas A. Bergman,[†] Dianne Alewood,[†] Shu-Hong Hu,[†] Paul F. Alewood,[†] Christopher J. Birch,*[,§] Jennifer L. Martin,*[,†] and David P. Fairlie*[,†]

Centre for Drug Design and Development, The University of Queensland, Brisbane, Queensland 4072, Australia, Victorian Infections Diseases Reference Laboratory, Private Bag 815, Carlton South, Victoria 3053, Australia, and Sir Albert Sakzewski Virus Research Centre, The Royal Children's Hospital, Herston, Queensland 4029, Australia

Received January 13, 2000

Three new peptidomimetics (**1**−**3**) have been developed with highly stable and conformationally constrained macrocyclic components that replace tripeptide segments of protease substrates. Each compound inhibits both HIV-1 protease and viral replication (HIV-1, HIV-2) at nanomolar concentrations without cytotoxicity to uninfected cells below 10 μM. Their activities against HIV-1 protease (K_i 1.7 nM (**1**), 0.6 nM (**2**), 0.3 nM (**3**)) are 1−2 orders of magnitude greater than their antiviral potencies against HIV-1-infected primary peripheral blood mononuclear cells (IC_{50} 45 nM (**1**), 56 nM (**2**), 95 nM (**3**)) or HIV-1-infected MT2 cells (IC_{50} 90 nM (**1**), 60 nM (**2**)), suggesting suboptimal cellular uptake. However their antiviral potencies are similar to those of indinavir and amprenavir under identical conditions. There were significant differences in their capacities to inhibit the replication of HIV-1 and HIV-2 in infected MT2 cells, **1** being ineffective against HIV-2 while **2** was equally effective against both virus types. Evidence is presented that **1** and **2** inhibit cleavage of the HIV-1 structural protein precursor $Pr55^{gag}$ to p24 in virions derived from chronically infected cells, consistent with inhibition of the viral protease in cells. Crystal structures refined to 1.75 Å (**1**) and 1.85 Å (**2**) for two of the macrocyclic inhibitors bound to HIV-1 protease establish structural mimicry of the tripeptides that the cycles were designed to imitate. Structural comparisons between protease-bound macrocyclic inhibitors, VX478 (amprenavir), and L-735,524 (indinavir) show that their common acyclic components share the same space in the active site of the enzyme and make identical interactions with enzyme residues. This substrate-mimicking minimalist approach to drug design could have benefits in the context of viral resistance, since mutations which induce inhibitor resistance may also be those which prevent substrate processing.

Introduction

Inhibitors of the human immunodeficiency virus type 1 (HIV-1) protease (HIV PR)[1−7] act by blocking the cleavage of HIV-1 precursor proteins $Pr55^{gag}$ and $Pr160^{gag-pol}$. The former is the precursor to the matrix (p17), capsid (p24), and nucleocapsid (p9) structural proteins, while the latter is the precursor to the viral enzymes reverse transcriptase (RT), RNase H, and the protease itself.[8] Although HIV PR inhibitors act late in the replication cycle of HIV-1 in acutely or chronically infected cells, they ultimately prevent early replicative events in newly infected cells, since their activity ensures that RT and RNase H are not available for the reverse transcription process and that mature p17 is not present as part of the preintegration complex.[9,10]

Combination therapy using inhibitors of both HIV RT and PR has played an important role in the success of highly active antiretroviral therapy (HAART).[11,12] Clinical trials have shown that many HIV-infected individuals undergoing HAART have rapid and profound reductions in plasma viral load, which can often be sustained for months or years. Unfortunately, suboptimal inhibitor concentrations in some patients often result from the difficulty in adherence to long-term dosing with multiple antiretroviral drugs or from patient-to-patient differences in pharmacokinetic drug profiles, inevitably leading to development of drug resistance. This is particularly problematic with clinical and preclinical protease inhibitors, with resistance to one often resulting in cross-resistance to others,[13] and inhibitors of other HIV proteins.[14] In reality there is really only a single protease inhibitor option available to most patients, highlighting the need for new drugs which either select for HIV with uncommon resistance-inducing mutations in the protease or overcome resistance altogether. Novel strategies for the design of such antiretroviral drugs in general and protease inhibitors in particular are clearly needed.

We now report the synthesis, stability, activities, and structures of new compounds (**1**−**3**) containing cyclic

* Address correspondence to D.P.F. (e-mail, d.fairlie@mailbox.uq.edu.au; fax, +61733651990), J.L.M. (e-mail, j.martin@mailbox.uq.edu.au), or C.J.B. (e-mail, Chris.Birch@mh.org.au).
[†] The University of Queensland.
[§] Victorian Infections Diseases Reference Laboratory.
[‡] The Royal Children's Hospital.

10.1021/jm000013n CCC: $19.00
Published on Web 08/25/2000

replacements for tripeptide sequences. We have demonstrated before in other molecules that such cyclic components are preorganized in a high-affinity protease-binding conformation[15−17] yet are flexible enough to potentially adapt to changes in the shape of the inhibitor-binding groove of the protease which occur as a result of drug-induced mutations. This report is part of a wider strategy to mimic protease substrates more closely than do current protease inhibitors and, in so doing, perhaps minimize the likelihood of viral resistance since only protease mutations that block or modulate substrate processing are likely to prevent substrate-mimicking inhibitors from binding to the protease. As a penultimate step toward this ultimate goal, we have here appended cyclic tripeptide mimics to some nonpeptidic moieties that help to confer potent HIV-1 protease inhibitor activity and antiviral activity at nanomolar concentrations.

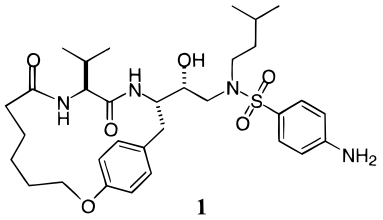

1

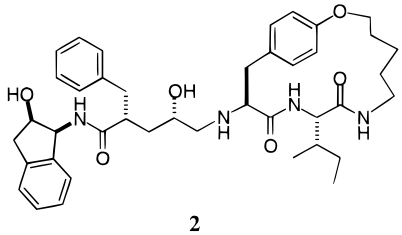

2

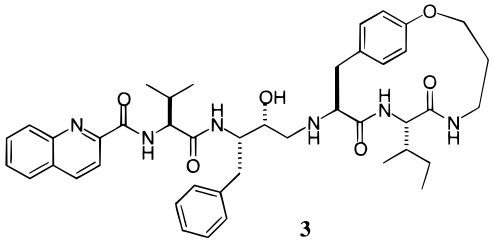

3

Results and Discussion

Protease Inhibitors. Compounds **1**−**3** each contain a cyclic component designed to function as a replacement for a P3−P1 or P1′−P3′ tripeptide segment of a substrate for HIV PR. Inhibitor **1** is a pentapeptide mimetic consisting of a 17-membered N-terminal macrocycle[15] designed to mimic an N-terminal tripeptide sequence Xaa-Val-Phe (P3−P1), a hydroxyethylamine isostere to mimic the transition state of peptide hydrolysis, and a nonpeptidic C-terminal *N*-isobutyl *p*-aminobenzenesulfonamide moeity (P1′−P2′) which is an analogue of the C-terminus of another HIV-1 PR inhibitor VX-478 (amprenavir),[18] but with an extra methylene inserted in the alkyl chain of **1** at P1′. Inhibitor **2** is also a pentapeptide mimetic, which links a C-terminal 17-membered macrocycle[16] designed to mimic a C-terminal tripeptide sequence Phe-Ile-Xaa (P1′−P3′) with a hydroxyaminopentanamide isostere to mimic the transition state of peptide hydrolysis and a nonpeptidic hydroxyaminoindan N-terminus (*N*-(2(*R*)-hydroxy-1(*S*)-indanyl)-2(*R*)-(phenylmethyl)-) that has previously been reported to occupy P2 and P1 in L-735,524 (indinavir).[19] Inhibitor **3** is a hexapeptide mimetic,[16] with a similar C-terminal macrocycle as in **2** and with the same N-terminus as in Ro31-8959 (saquinavir).[20]

Using our reported syntheses[21] for the epoxide derivative **6** of the N-terminal macrocyclic component of **1** (namely **4**) and for the amine derivatives[21] **5** and **9** of the C-terminal cycle in both **2** and **3**, it was a straightforward exercise to construct inhibitors **1**−**3** by appending these to the appropriate acyclic components (Schemes 1, 2). The compounds were purified by reversed-phase HPLC and fully characterized by ^{1}H NMR spectroscopy and high-resolution mass spectrometry.

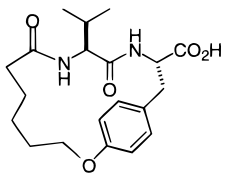

4

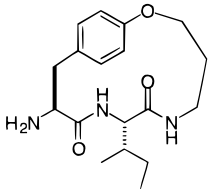

5

Compounds **1**−**3** were evaluated as inhibitors of synthetic HIV-1 PR at pH 6.5 (I = 0.1 M) as described in Materials and Methods. They had K_i values of 1.7, 0.6, and 0.3 nM, respectively, versus 1.8 nM for JG365[16] and 1.0 nM for DMP323[16] under the same conditions.

Scheme 1

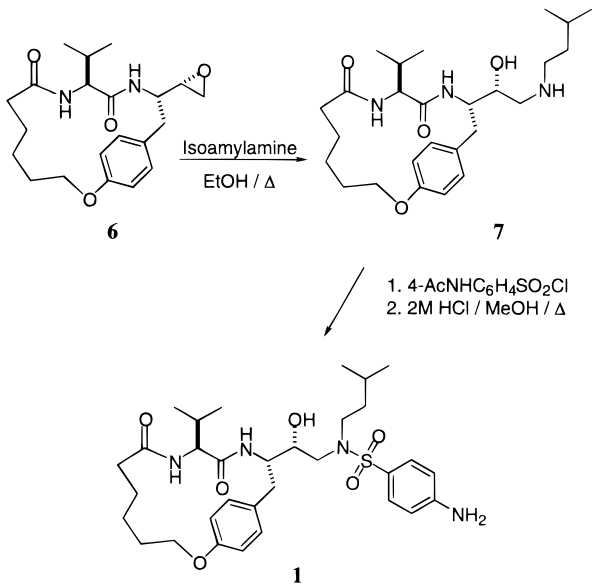

6 **7** **1**

Macrocycle Stability. To investigate whether the cyclic peptide components of these inhibitors were proteolytically stable toward mammalian proteases that are likely to be encountered in vivo, compounds **4** and **5** were exposed to various degradative proteases found in the GI tract, plasma or in cells. The macrocycles were completely stable in 3 M hydrochloric acid at 40 °C over 5 days with no sign of any decomposition as assessed by rpHPLC and electrospray MS. When incubated at 37 °C for up to 24 h with either (a) selected gastric, plasma, or cellular proteases, (b) gastric juice from rat stomachs, (c) serum (1-h incubation only), or (d) contents

Scheme 2

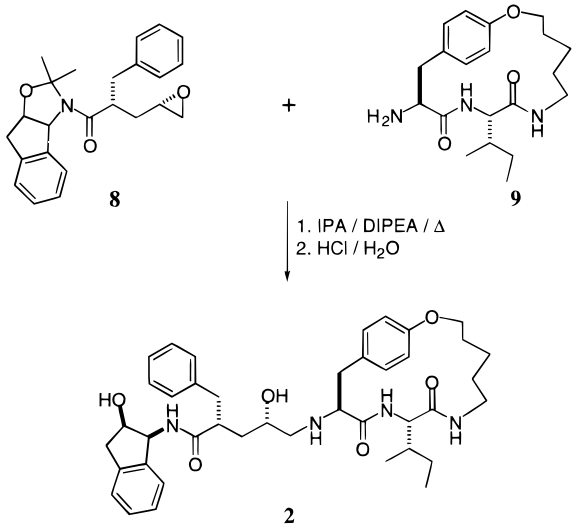

of lysed human lymphocytes, monocytes, or polymorphonuclear leukocytes, there were similarly no indications of decomposition of the macrocycles. Under the same conditions, control linear peptides (e.g. AcLVF-{ψ(CHOHCH$_2$)}-FIV-NH$_2$ and YSFKDMQLGR) were completely hydrolyzed (100%) within minutes.

The results are summarized in Materials and Methods and indicate that the macrocycles confer important properties on the peptidomimetics. Although the cycles contain two amide bonds, they are not susceptible to hydrolytic/proteolytic cleavage like normal peptide bonds.

Antiviral Activity. Compounds **1**−**3** were tested for antiviral activity by investigators in two different cities, and each was found to be a potent inhibitor of the replication of HIV-1 in acutely infected cells (Table 1). We found that for cord blood mononuclear cells (CBMC) infected with HIV-1 (strain TC354, SASVRC, Brisbane), IC_{50} values were 45 nM (**1**, $n = 5$), 56 nM (**2**, $n = 5$), and 95 nM (**3**, $n = 5$). Studies were also undertaken using primary peripheral blood mononuclear cells and MT2 cells infected with a different strain of HIV-1 (#237288, a laboratory-adapted, syncytial-inducing strain isolated from an AIDS patient at Fairfield Hospital, Melbourne). An example of these latter results (Table 1) is the data for MT2 cells in which IC_{50} was 90 nM (IC_{90} 0.22 μM) for **1** and 60 nM (IC_{90} 0.10 μM) for **2**. No drug-induced cytotoxicity was observed below 10−50 μM. These compounds thus have significant activity against HIV-1 at concentrations that are not toxic to cells.

Complete inhibition of viral replication occurred at concentrations significantly lower than those which were cytotoxic, thereby resulting in selective indices (SIs) of 45 and 57 for **1** in MT2 and PBMCs, respectively, and 300 and 227 for **2** in the same cell types (Table 1). These results compare very favorably with those for indinavir under the same conditions (Table 1, SI = 107). However, while compound **2** had comparable activity against HIV-2 in acutely infected MT2 cells (SI of 176), compound **1** had only marginal activity against the same strain of HIV-2 (SI = 2.0; Table 2).

To check that these new macrocyclic compounds were exerting their antiviral activity via the anticipated protease inhibition mechanism rather than some other process, **1** and **2** were examined for inhibition of the cleavage of the HIV-1 structural protein precursor Pr55^{gag} in virions derived from chronically infected HqHTLV-IIIB cells. In the absence of inhibitors, these cells produced virions containing low levels of the precursor but substantial amounts of its product p24, indicating that protease-directed cleavages occur as expected in these viruses (Figure 1, lane 2). In virions produced from cells treated with either **1** or **2**, there was evidence of inhibition of protease-directed cleavage (Figure 1, lanes 3 and 4). Uncleaved Pr55^{gag} was present in virions derived from both sources. Nevertheless, some cleavage of Pr55^{gag} did occur in the presence of either

Table 1. Antiviral Activity and Cytotoxicity of **1**−**3** in PBMCs and MT2 Cells Infected with HIV-1

drug	cell	CC_{10}[a] (μM)	IC_{50}[b] (μM)	IC_{90}[c] (μM)	SI[d]
1	CBMC[e]		0.045		
	PBMC[f]	50.0	0.43	0.88	57
	MT2[f]	10.0	0.09	0.22	45
2	CBMC[e]		0.056		
	PBMC[f]	50	0.11	0.22	227
	MT2[f]	30.0	0.06	0.10	300
3	CBMC[e]		0.095		
DMP323	CBMC[e]		0.110		
amprenavir	MT2[f]	10.0	0.03	0.08	125
indinavir	PBMC[f]	10.0	0.052		
	MT2[f]	10.0	0.056	0.093	107.5

[a] CC_{10}: concentration of inhibitor causing death in 10% or less of cells in the absence of virus. [b] IC_{50}: concentration of inhibitor producing a 50% decrease in virion-associated RT activity relative to untreated, infected control. [c] IC_{90}: concentration of inhibitor producing a 90% decrease in virion-associated RT activity relative to untreated, infected control. [d] SI (selective index) = CC_{10} divided by IC_{90}. [e] HIV-1 strain TC354 (Brisbane). [f] HIV-1 strain 237288 (Melbourne).

Table 2. Cytotoxicity and Inhibitory Concentrations of **1** and **2** in MT2 Cells Infected with HIV-2[a]

drug	CC_{10}[b] (μM)	IC_{50}[c] (μM)	IC_{90}[d] (μM)	SI[e]
1	10.0	0.50	5.0	2.0
2	30.0	0.10	0.17	176

[a] Strain of HIV-2 is ROD. [b] CC_{10}: concentration of inhibitor causing death in 10% or less of cells in the absence of virus. [c] IC_{50}: concentration of inhibitor producing a 50% decrease in virion-associated RT activity relative to untreated, infected control. [d] IC_{90}: concentration of inhibitor producing a 90% decrease in virion-associated RT activity relative to untreated, infected control. [e] SI (selective index) = CC_{10} divided by IC_{90}.

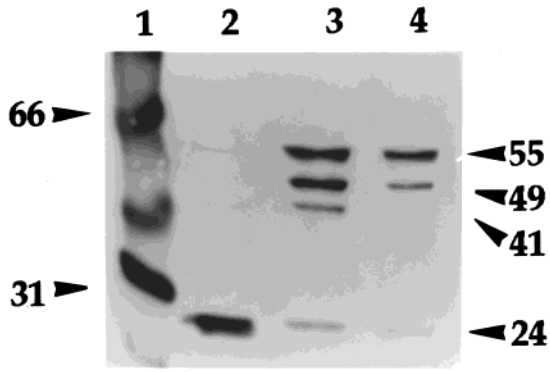

Figure 1. Immunoblot of HIV virions produced from H9/HTLV-IIIB cells after 72-h exposure to either no drug (lane 2) or 10 μM of either **1** (lane 3) or **2** (lane 4). Standard molecular weight markers (kD) are present in lane 1. The HIV structural precursor protein Pr55^{gag}, two of its cleavage intermediates (of molecular weight 49 and 41 kD), and the product p24 are indicated.

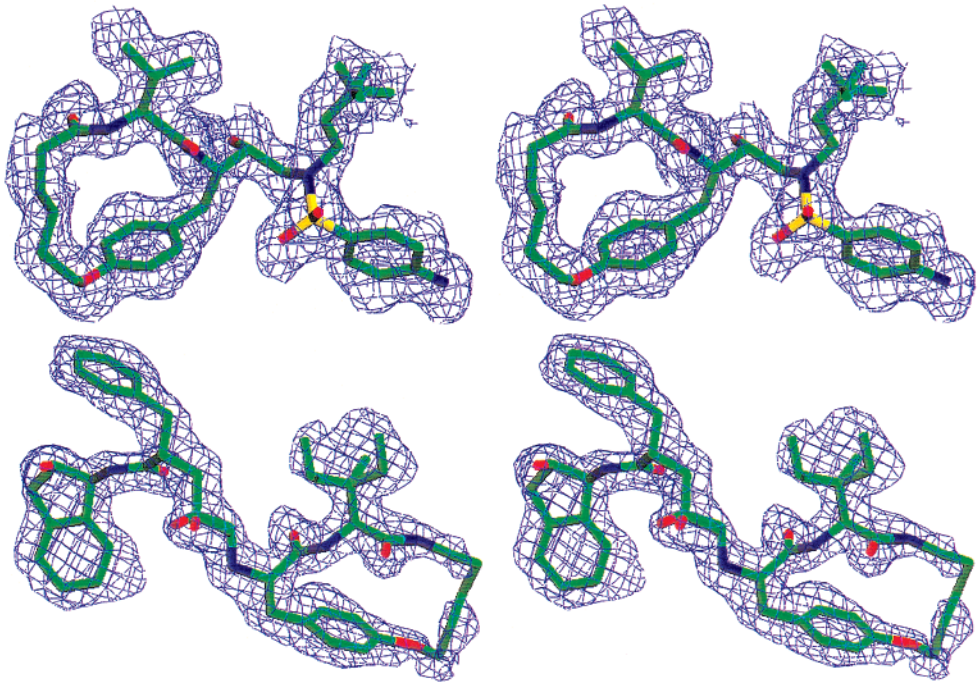

Figure 2. Stereoview of electron density maps for **1** and **2** bound to HIV-1 PR. The $2F_o - F_c$ maps are shown, contoured at 1.0σ.

inhibitor, indicated by the increased amounts of 49- and/or 41-kD intermediates compared to that in virions derived from untreated cells. However, subsequent cleavage of these intermediates to the p24 product was substantially inhibited in virions exposed to either drug, consistent with protease inhibition being responsible for their antiviral activity.

Crystal Structures. Inhibitors **1** and **2** were cocrystallized with synthetic HIV-1 PR containing the mutations Q7K, L33I, C37Aba, and C95Aba (Aba = α-aminobutyric acid). The cysteine residues were replaced for easier synthesis and handling, while the two autocleavage sites (Q7, L33) were mutated to reduce autolysis.[22] The synthetic mutant [Lys^7,Ile^{33},Aba^{67,95}]-HIV-1 PR is designated HIVKI, and its enzymatic properties have been fully characterized elsewhere.[9,23] Both complexes crystallized in the space group $P2_12_12_1$ in a crystal form isomorphous with the HIV-1 PR:JG-365 complex.[24] The inhibitor electron density observed in both structures (Figure 2) was in excellent agreement with the composition of inhibitors **1** and **2**.

The crystal structure of **1** shows that carbonyl oxygens and NH groups of both amides in the macrocycle form hydrogen bonds with the enzyme (Figure 3), and these hydrogen bonds are equivalent to those observed in acyclic peptidic inhibitor complexes. Also, the aromatic ring (P1) and isopropyl (P2) and pentyl (P3) groups of the macrocycle in **1** occupy similar positions in the enzyme as the side chains of Phe/Tyr, Val/Asn, and Nle, respectively, from acyclic peptidic inhibitors that complex in the active site of HIV-1 PR. The aliphatic pentyl chain in the macrocycle of **1** (C1−C5) is more disordered than the rest of the inhibitor with an average *B* factor of ∼21 Å^2 for the five carbon atoms compared to ∼15 Å^2 for other inhibitor atoms. The methylene group (C2) of the aliphatic chain appears to make an unfavorable contact (3.3 Å) with Arg108 Nη_2, while at the opposite end of the active site the corresponding Arg8 Nη_2 also approaches closely (within 3.9 Å) to C26 of the flexible P1′ isoamyl group of **1**.

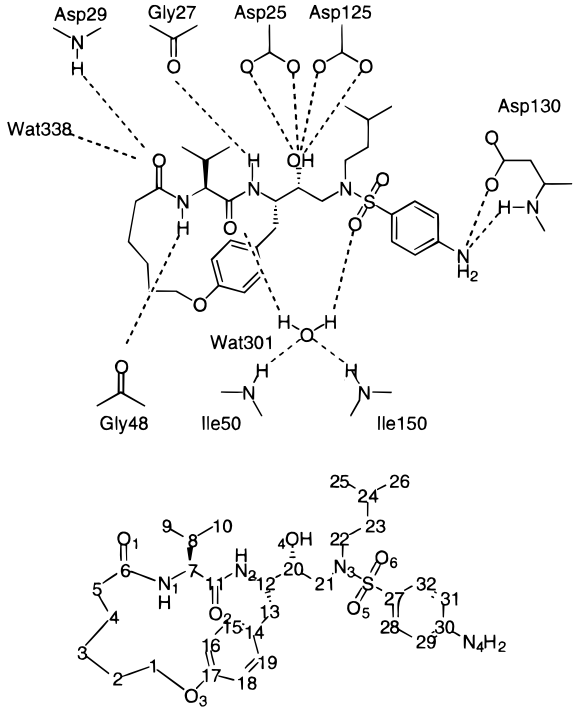

Figure 3. Hydrogen-bonding interactions between HIV-1 PR and **1** (top), with the corresponding inhibitor-numbering system below.

The hydroxyl group of **1** forms hydrogen bonds with both catalytic aspartates (Figure 3), as observed for most protease inhibitors containing this transition-state isostere. The C-terminal *N*-alkylsulfonamide makes interactions with the enzyme that are similar to those observed for the alkylsulfonamide of VX-478.[18] Specifically, a sulfonyl oxygen (O5) interacts with Wat301 which in turn hydrogen-bonds to the amide nitrogens of flap residues Ile50 and150. The other sulfonyl oxygen

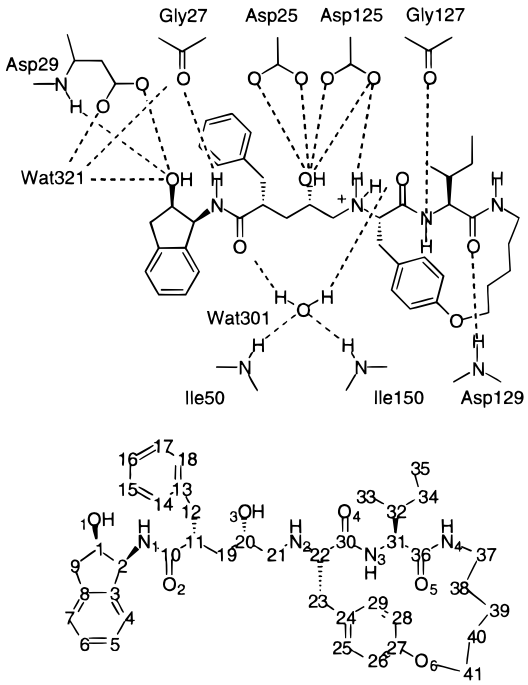

Figure 4. Hydrogen-bonding interactions between HIV-1 PR and **2** (top), with the corresponding inhibitor-numbering system below.

(O6) is close to side chains of Ile50 (Cδ 3.5 Å) and Ile184 (Cδ 3.5 Å). The isoamyl group of P1′ is flexible (two conformations were modeled) and interacts with side chains of Leu23, Pro81, Val82, and Ile184. The *para*-amino substituent is within hydrogen-bonding distance of the amide nitrogen and oxygen of Asp130.

The crystal structure of **2** bound to HIV-1 PR shows that the nonpeptidic N-terminal end and transition-state isostere interact with the enzyme in the same way as for L-735,524. The extra methylene in the transition-state isostere of **2** compared with that in **1** imparts added flexibility to this region, permitting two alternative isostere conformations to be modeled in the crystal structure. Both conformations enable the hydroxyl group to interact with both enzyme catalytic aspartates. The extra methylene also causes a C-terminal translation of the inhibitor along the active site groove compared with **1**, so that the aliphatic hydrocarbon linker in the macrocycle becomes solvent accessible and somewhat disordered. This is in contrast to other inhibitors that incorporate an hydroxyethylamine isostere linked to a C-terminal macrocycle, which are all translated toward the N-terminus and have well-ordered macrocycles.[22] However, the HIV PR:**2** complex retains the interaction between the protonated secondary amine (N2) and catalytic aspartate (2.9 Å), as well as hydrogen bonds with the Phe amide CO and Ile CO and NH atoms of **2** (Figure 4), as observed in crystal structures of other

Table 3. Crystallographic Parameters and Data Processing Statistics

	1	**2**
resolution (Å)	1.75	1.85
a (Å)	51.4	51.8
b (Å)	58.8	58.9
c (Å)	61.7	61.9
R_{sym}[a]	0.083	0.051
(in top shell)	(0.302)	(0.277)
completeness (%)	94.5	92.7
(in top shell (%))	(84.6)	(87.9)
$I/\sigma I$	9.5	12.0
(in top shell)	(2.1)	(2.9)
no. obsd ($I/\sigma I > 1$)	59019	51287
no. unique reflns	18470	15546
top resolution shell (Å)	1.83−1.75	1.92−1.85

[a] $R_{sym} = \Sigma_h(I_h - \langle I_h \rangle)/\Sigma\langle I_h \rangle$.

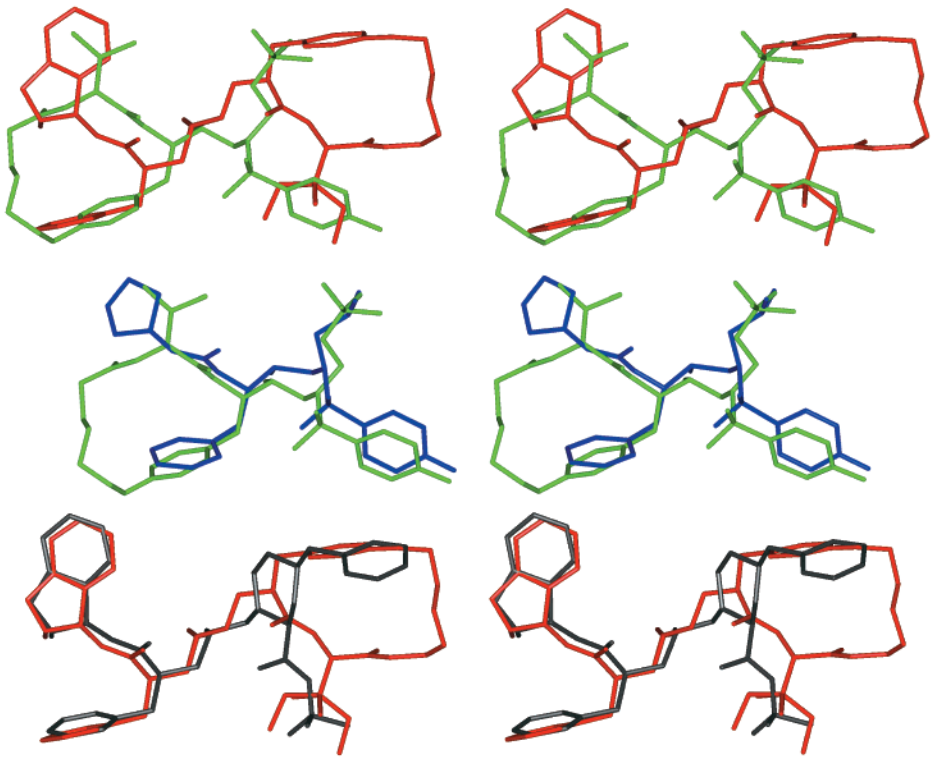

Figure 5. Superimposition of (top) **1** (green) and **2** (red), (middle) **1** and VX-478 (blue), and (bottom) **2** and L-735,524 (gray).

inhibitors with C-terminal macrocycles bound to HIV-1 PR.

The isoleucine side chain of **2** is flexible, permitting two inhibitor conformations to be modeled, and has hydrophobic interactions with Ile50, Ala128, Val132, and Ile184 side chains in the S2′ pocket. As for the complex with **1**, unfavorable contacts occur between Arg8 Nη_1 and **2** (macrocycle C40, 3.0 Å; benzyl ring C28, 3.1 Å). A third unfavorable interaction occurs between Arg108 Nη_1 and C17 of the phenylalanyl substituent of **2**. Although Wat301 forms the usual hydrogen bonds between the inhibitor and the flap nitrogens in the HIV PR:**2** complex, it is less ordered than in other HIV PR complexes. The *B*-factor of Wat301 in the HIV PR:**2** complex is high (28 Å^2) compared with the corresponding water in the complex with **1** (∼9 Å^2) and the two waters are ∼0.5 Å apart. In the active site of the protease three of the four hydrogen bonds of Wat301 are lengthened (0.2−0.4 Å) in the complex with **2**. The two equivalent acceptor atoms that interact with Wat301 in the P1′ site (O6 of **1** and O4 of **2**) are 2.2 Å apart. There may be several reasons for this. The constrained cycle of **2**, in conjunction with the isoleucyl residue at S2′, forces the tyrosinyl group deep into the S1′ pocket (Figure 5, red, top). Thus the nature of the substituents in the S1′ and S2′ sites dictate the position of these acceptor atoms. The sulfonyl oxygen (O5), **1**, is closer to Wat301 (by 0.4 Å) than the corresponding carbonyl donor of **2** (O4), due to the sulfonamide group puckering toward the flap region. However, this puckering also has the effect of pushing the enzyme flaps into a more open position. In both crystal structures reported here the main chain atoms of Ile150 and Gly151 are modeled with two alternate conformations. This observation has been described previously.[22] One difference in these two structures is that the corresponding residues in the opposite flap, Ile50 and Gly51, have only one conformation. Furthermore, the conformation observed in the complex with **1** is opposite to that observed in the complex with **2**.

Figure 5 compares in stereo the bound conformations of **1** and **2** with that of their corresponding acyclic inhibitors, VX-478 (middle, rmsd 0.55 Å) and L-735,524 (bottom, rmsd 0.47 Å), respectively. Both macrocyclic inhibitors bind in a fashion similar to the equivalent parts of the acyclic drugs. The isosteric hydroxyl groups of **1** and **2** are separated from the hydroxyls of the acyclic inhibitors by 0.5 Å (middle) and 0.2 Å (or 0.7 Å for the alternate conformation, bottom), respectively. The tertiary nitrogen of the sulfonamide group, **1**, is shifted by ∼1 Å compared with VX-478 due to the addition of an extra methylene group in the alkyl chain (middle). Tables 5 and 6 also demonstrate that the hydrogen-bonding distances between analogous acyclic portions of the inhibitor−enzyme complexes for **1** versus amprenavir (Table 5) and **2** verus indinavir (Table 6) are similar. Clearly the binding modes of these nonpeptidic acyclic portions are very similar.

Summary

Three new compounds (**1**−**3**) containing 15−17-membered macrocycles have been found to potently inhibit (a) processing of a synthetic peptide by HIV-1 PR, (b) intracellular processing of a gag-pol polypeptide in HIV-1-infected cells, and (c) replication of two different viral strains of HIV-1 in infected primary and cultured lymphocytes. The macrocycles confer a number of valuable properties. They are structural mimics of tripeptides fixed in the extended strand conformation that is now known[25,40] to be crucial for recognition by all proteases, including HIV-1 PR. The crystal structures show that the cycles position their two amides precisely to form the same hydrogen-bonding patterns as acyclic peptides. The macrocycles also permit orientation of side chains into the same three-dimensional space occupied by the corresponding side chains of acyclic peptides leading to identical protease−inhibitor interactions. Together with previous results,[15−17,22] it is now clear that this novel class of inhibitors can be translated along the active site through modification of the length and charge state of the transition-state isostere.

Unlike the tripeptide segments that they mimic, the

Table 4. Refinement Statistics for the HIV-1 PR:Inhibitor Complexes

	1	**2**
resolution range (Å)	8−1.75	8−1.85
no. protein atoms[a]	1542	1530
no. inhibitor atoms[a]	45	58
no. waters	121	89
no. sulfate atoms	3 × 5	2 × 5
reflections (F >0σ (F))	18244	15323
R-factor[b]	0.189	0.212
(top shell)[c]	(0.288)	(0.288)
R-free[d]	0.231	0.259
(top shell)[c]	(0.323)	(0.312)
rms ideal bond length (Å)	0.009	0.005
rms ideal bond angle (deg)	1.48	1.16
coordinate error (Å)[e]	0.20−0.25	0.24−0.28
⟨*B*⟩ all atoms (Å^2)[f]	19.5	24.5
⟨*B*⟩ inhibitor atoms (Å^2)[f]	15.3	22.3

[a] Including alternative conformations. [b] $R = \Sigma|F_o - F_c|/\Sigma F_o$. [c] Top resolution shell (Å): 1.83−1.75, **1**; 1.93−1.85, **2**. [d] Cross-validation *R*-factor using 10% of data. [e] Ref 42. [f] ⟨*B*⟩: average *B*-factor.

Table 5. Corresponding Hydrogen-Bonding Interactions between Acyclic Components of Inhibitors **1** and Amprenavir with HIV-1 PR (cutoff 3.3 Å)

		distances (Å)	
inhibitor atom	protein residue	**1**	amprenavir
O4H	Asp25 Oδ_1	3.1	3.1
O4H	Asp25 Oδ_2	2.8	2.6
O4H	Asp125 Oδ_1	2.8	2.8
O4H	Asp125 Oδ_2	2.7	2.7
O5	Wat301	2.7	2.8
N4H	Asp130 Oδ	3.1	3.2
N4H	Asp130 NH	3.3	3.2

Table 6. Corresponding Hydrogen-Bonding Interactions between Acyclic Components of Inhibitors **2** and Indinavir with HIV-1 PR (cutoff 3.3 Å)

		distance (Å)	
atom	protein residue	**2**	indinavir
O1H	Wat321	3.1	2.8
O1H	Asp29 O	3.0	3.1
O1H	Asp29 NH	3.3	3.2
N1H	Gly27 C=O	3.3	3.0
O2	Wat301	3.0	2.8
O3H	Asp25 Oδ_1	2.8 (2.8)[a]	2.6
O3H	Asp25 Oδ_2	3.1 (3.0)[a]	3.0
O3H	Asp125 Oδ_1	3.3 (2.7)[a]	2.9
O3H	Asp125 Oδ_2	3.0 (2.9)[a]	2.8

[a] Denotes second conformation.

macrocycles are stable for at least 24 h at 37 °C to 3 M HCl and to gastric, plasma, and cellular proteases under conditions where linear peptides are completely degraded within minutes. This greater stability suggests that the macrocycles should survive all proteolytic conditions encountered during oral delivery, plasma circulation, and cellular localization. The two crystal structures reported here, together with others for this class of inhibitor, also support the idea that nonpeptidic units can be attached to the macrocycles without loss of protease activity. Indeed this may be a useful means of regulating antiviral activity, membrane permeability, oral bioavailability, and pharmacokinetic and toxicological properties of these drugs.

Our results show that the antiviral activity of these macrocyclic peptidomimetics against HIV-1 involves a mechanism characteristic of inhibition of HIV-1 PR. All three compounds inhibit replication of HIV-1 to a similar extent as does indinavir. Compound **2** was also active in preventing replication of HIV-2, contrasting with the poor activity of **1** against the same virus. In light of the development of clinical resistance to HIV PR inhibitors and the issue of cross-resistance, the availability of novel inhibitors of HIV PR is becoming increasingly important. Although not reported here, we have had difficulty in generating resistance to **1** and **2** in vitro and are examining the efficacy of these drugs against clinical isolates of HIV-1 known to be resistant to HIV-1 PR inhibitors that have been approved for human use. In view of its structural similarity to peptide substrates, this macrocyclic class of HIV PR inhibitor is very promising because HIV PR mutations that reduce inhibitor affinity may also be expected to reduce substrate processing.

Materials and Methods

1. Inhibitor Synthesis and Characterization. (10*S*,-13*S*,1′*R*)-13-[1′-Hydroxy-2′-(*N*-*p*-aminobenzenesulfonyl-1″-amino-3″-methylbutyl)ethyl]-8,11-dioxo-10-isopropyl-2-oxa-9,12-diazabicyclo[13.2.2]nonadeca-15,17,18-triene (1). The amine **7** and 4-acetamidobenzenesulfonyl chloride were dissolved in THF:H_2O (4:1) and diisopropylethylamine was added (Scheme 1). After 10 min the solution was diluted with EtOAc and washed with 2 M HCl. The solvent was evaporated and the residue was dissolved in MeOH and 2 M HCl and refluxed for 2 h. The solution was basified with 10% K_2CO_3 and extracted with EtOAc. The EtOAc extracts were washed with brine and dried over $MgSO_4$ and evaporated. The residue was purified by flash chromatography (SiO_2, 100% EtOAc) giving **1** as a white powder: R_f 0.42 (100% EtOAc); ^{1}H NMR (300 MHz, CD_3OH) δ 7.92 (d, J = 9.7 Hz, 1H, Tyr-NH), 7.51 (m, 2H, $J_{AX} + J_{AX'}$ = 8.7 Hz, ortho to SO_2), 7.19 (d, J = 9.2 Hz, 1H, Val-NH), 7.07 (m, 2H, $J_{AX} + J_{AX'}$ = 8.5 Hz, ortho to CH_2), 6.77 (m, 2H, $J_{AX} + J_{AX'}$ = 8.5 Hz, ortho to O), 6.73 (m, 2H, $J_{AX} + J_{AX'}$ = 8.7 Hz, ortho to NH_2), 4.27−4.05 (m, 3H, Tyr-αH and H-3), 4.07 (dd, J = 9.2, 6.0 Hz, 1H, Val-αH), 3.75 (m, 1H, H-1′), 3.40 (dd, J = 14.3, 4.0 Hz, H-2′), 3.35−3.02 (m, 2H, H-4′), 3.18 (dd, J = 13.6, 3.7 Hz, 1H, H-14), 2.93 (dd, J = 14.3, 8.6 Hz, H-2′), 2.41 (dd, J = 13.2, 12.5 Hz, 1H, H-14), 2.20−2.11 (m, 2H, H-7), 1.86 (m, 1H, Val-βCH), 1.75−1.60 (m, 2H), 1.60−1.10 (m, 7H), 0.87 (d, J = 6.4 Hz, 9H, Val-γCH_3, H-7′, H-8′), 0.76 (d, J = 6.8 Hz, 3H, Val-γCH_3); ^{13}C NMR (CD_3OD) δ 174.8, 172.6, 158.3, 154.3, 131.4, 130.3, 117.4, 114.5, 74.2, 68.8, 58.6, 55.0, 53.1, 38.2, 36.1, 36.0, 33.5, 30.7, 27.1, 26.1, 22.9, 22.8, 20.0, 18.2; HRMS *m/e* 616.3285 calcd for $C_{32}H_{48}N_4O_6S$ 616.3295.

***N*-13-[(10*S*,13*S*)-9,12-Dioxo-10-(2-butyl)-2-oxa-8,11-diazabicyclo[13.2.2]nonadeca-15,17,18-trienyl]-(2*R*)-benzyl-(4*S*)-hydroxy-5-aminopentanoic-(1*R*)-hydroxy-(2*S*)-indaneamide (2).** A solution of the macrocyclic amine **9** (220 mg, 0.61 mmol, 2.4 equiv) and the chiral, optically active epoxide **8** (93 mg, 0.25 mmol) in 2-propanol (3 mL) and diisopropylethylamine (200 mL) was stirred and refluxed for 14 h (Scheme 2). Hydrochloric acid (2 M, 2 mL) and MeOH (5 mL) were added and heating was continued for 30 min. The solution was evaporated to dryness and the residue was purified by RP HPLC (A: 0.1% TFA in H_2O, B: 0.1% TFA in 90/10 MeCN/H_2O 30-min gradient to 40:60% B), retention time 30 min, giving **2** as a white powder (130 mg, 75%) after lyophilization: ^{1}H NMR (500 MHz, CD_3OH) δ 7.83 (d, J = 8.5 Hz, 1H, NH), 7.78 (m, 1H, CH_2NH), 7.70 (d, J = 7.5 Hz, NH), 7.33−7.15 (m, 9H, Ar), 7.05 (m, 2H), 6.83 (m, 2H), 5.25 (dd, J = 8.5, 5.0 Hz, 1H), 4.36 (m, 1H), 4.31−4.25 (m, 1H), 4.20 (dd, J = 11.6, 5.7 Hz, 1H), 4.14 (m, 1H), 3.96 (m, 1H), 3.87 (dd, J = 7.5, 5.5 Hz, 1H), 3.58−3.49 (m, 1H), 3.28 (dd, J = 12.7, 5.5 Hz, 1H), 3.12 2.66 (m, 10H), 1.90 (m, 1H), 1.82−1.65 (m, 2H), 1.59−1.33 (m, 6H), 1.32−1.21 (m, 1H), 1.05 0.94 (m, 1H), 0.86 (t, J = 7.4 Hz, Ile-γCH_3), 0.81 (d, J = 6.8 Hz, Ile-βCH_3); ^{13}C NMR (CD_3OD) δ 177.4, 171.0, 167.1, 159.4, 142.2, 141.8, 140.3, 131.4, 130.2, 129.6, 128.9, 127.9, 127.6, 126.9, 126.2, 125.3, 117.2, 74.0, 67.9, 66.4, 63.5, 59.2, 58.7, 53.4, 46.1, 40.8, 40.6, 40.2, 39.2, 39.0, 38.0, 36.4, 29.5, 29.3, 26.6, 23.7, 15.2, 12.1; HRMS *m/e* 698.4059 calcd for $C_{41}H_{54}N_4O_6$ 698.4043.

Compound **3** was prepared and characterized as described elsewhere.[16]

2. Protease Inhibition. [Aba^{67,95}]HIV-1 PR (SF2 sequence) was chemically synthesized by a solid-phase method as described[26] and is kinetically characterized elsewhere using a fluorometric assay[27] to quantify its activity. Cleavage of the substrate 2-aminobenzoyl-Thr-Ile-Nle-(*p*-nitroPhe)-Gln-Arg-NH_2 releases a fluorescent product (2-aminobenzoyl-Thr-Ile-Nle). Using appropriate buffer, substrate, ionic strength, diluents and pH, protease inhibition was determined by fluorescence using a Jasco FP-770 spectrofluorimeter.

3. Macrocycle Stability. Macrocycles **4** and **5** (50 μL of 1.0 mg in 1.0 mL of DMSO) were incubated for up to 24 h at 37 °C with 1 mL of aqueous buffer containing either pepsin, gastricsin, trypsin or chymotrypsin (0.3 mg in 3 mL; pH 2, 3, 8, 8, respectively). Aliquots (0.3 mL) were sampled at 1, 4, 24 h and quenched with aqueous base (10 μL of 1 M NaOH) before analysis by reversed-phase HPLC (50% acetontrile/50% water/0.1% TFA for 30 min then 100% acetonitrile 5 min) versus buffer alone. Fractions were monitored for peak identification by electrospray MS. There was no evidence for decomposition of the macrocycles under these conditions, whereas the linear peptide was completely degraded within 5 min.

The compounds were also separately incubated with gastric juice from stomachs of three Dark Agouti rats euthanized with nembutal. The stomach and gut were removed and washed with saline solution. A saline suspension of the GI tract was macerated and refrigerated (−20 °C) overnight to lyse the cells and release their contents. The solution was centrifuged (400*g*) and the supernatant diluted 1:3 into separate aqueous buffers (pH 2.2, glycine·HCl; pH 4.0, Mes, acetic acid; pH 6.0, NaMES). To each gastric/buffer solution (1 mL) was added 50 μL of compound stock from above or control linear peptide, and after incubation at 37 °C aliquots were taken at 1, 5, 24 h before adding 10 μL of 1 M NaOH and analysis by rpHLC and MS as above. Results indicate that both compounds were completely stable for at least 24 h in simulated conditions of the digestive tract.

Blood (3 mL) was collected by vena puncture and layered at room temperature onto a Ficoll density gradient solution 1077 (Histopaque-1077) in a ratio 1:1 in a heparinized 10-mL conical centrifuge tube. Histopaque-1077 is a mixture of polysucrose and sodium diatrizoate adjusted to a density of 1.077 ± 0.001 g/mL and facilitates rapid recovery of viable mononuclear cells from blood. After centrifugation (400*g*, 30 min, 22 °C), the upper plasma layer was aspirated with a Pasteur pipet to within 0.5 cm of the opaque interface containing mononuclear cells and discarded. The opaque interface was transferred to a clean tube, diluted with 10 mL of phosphate-buffered saline ($CaCl_2$ 0.9 mM, $MgCl_2$ 0.5 mM,

KCl 2.7 mM, KH_2PO_4 1.5 mM, NaCl 136.9 mM, Na_2HPO_4 3.2 mM), and aspirated by pipet. The solution was centrifuged (250*g*, 10 min), the supernatant discarded, the cell pellet resuspended in PBS (5 mL), and this washing procedure twice repeated. Using a Rapid Dif Kit, a thin film of cell solution was smeared onto microscope slides and treating with MeOH (5× to fix the cells), xanthene dye (5×), thiazene dye (1×), before examined cell types by microscopy. Cells were then successfully lysed by sonication (3 × 18 s) and centrifuged (2000*g*, 15 min) and the supernatant was collected.

PMNs were prepared from the original centrifugation with Histopaque-1077; the bottom layer containing the red cells was removed and exposed to hypotonic shock with cold distilled water (40s) to lyse the red blood cells, after which tonicity was restored with 10 N PBS. Cells were centrifuged (700*g*, 20 min) and the pellet was again exposed to hypotonic shock to remove residual red cells. Tonicity was restored, cells were centrifuged (700*g*, 20 min) and the pellet was resuspended in PBS. The cells were then lysed by sonication (3 × 18 s) and centrifuged and the supernatant was collected.

The lymphocyte and PMN solutions (1 mL) were incubated with **4**, **5** or control peptides (50 μL of 1 mg/mL DMSO stock solution) at 37 °C for 24 h and aliquots taken at 1, 24 h for analysis by RP HPLC and ESMS. Human serum and test compounds were similarly incubated and after 1 h the serum proteins were precipitated by addition of cold acetonitrile (1 mL). The samples were vortexed (30 s) and centrifuged (10000*g*, 5min), and the supernatant was analyzed as above.

4. Virology. Cells: Cord blood mononuclear cells (CBMC) were isolated by centrifugation of heparinized umbilical cord blood (Royal Brisbane Hospital) over Ficoll-paque. Phytohemagglutinin (PHA)-stimulated CBMC were prepared by culture of CBMC in RPMI 1640 supplemented with 20% heat-inactivated fetal calf serum (FCS), 2 mM glutamine, 100 U/mL penicillin and 100 μg/mL streptomycin (20FC/RPMI), with the addition of 0.2% (v/v) PHA for 3 days. PHA-CBMC were washed twice with 20FC/RPMI immediately prior to use. HIV-1 strain TC354 was propagated in PHA-CBMC in 20FC/RPMI supplemented with 20 U/mL recombinant interleukin-2.

MT2 and H9/HTLV-IIIB cells were obtained from the National Institutes of Health AIDS Research and Reference Program. PBMCs from individuals not infected with HIV were obtained from blood packs supplied by the Australian Red Cross Blood Bank, Melbourne. The medium used for passage and maintenance of MT2 and H9/HTLV-IIIB cells was RF10, an RPMI-1640-based medium.[28] RF10 supplemented with interleukin-2 (RF10/IL-2)[28] was used for experiments involving the use of PBMCs.

Anti-HIV activity of 1−3 in acutely infected CBMC lymphocytes: In these Brisbane studies PHA-CBMC were inoculated with HIV-1 (TC354) in the presence of 20 μg/mL diethylaminoethyl-dextran (DEAE-dextran) at a multiplicity of infection of 1 and allowed to adsorb for 2 h at 37 °C. Uninoculated PHA-CBMC were held as negative controls. Unbound virus was removed by washing three times with 20FC/RPMI. 10^5 Cells were placed in microtiter wells to which the appropriate dilutions of each test compound (in DMSO) or DMSO controls were added in triplicate. Culture medium (20FC/RPMI supplemented with 20 U/mL rIL-2) was added to make up the volume to 200 μL. Cultures were placed in an incubator at 37 °C (5% CO_2) for 3 days.

Virus replication was assessed by monitoring Day 3/4 culture supernatant for the presence of reverse transcriptase activity. 50 μL of reaction cocktail (20 μCi/mL ^{3}H-thymidine triphosphate, 50 mM Tris, ph 7.8, 75 mM KCl, 5 mM $MgCl_2$, 2 mM dithioreitol (DTT), 5 μg/mL poly-rA, 80 μg/mL dATP, 1.5 ng/mL oligo-dT, 0.05% Triton X-100) and 10 μL of culture supernatant were added to the appropriate wells of a microtiter plate and mixed gently and the plate was incubated (37 °C, 2 h). DE81 paper was marked with a labeled grid of rectangles measuring 0.9 cm × 3 cm and 10 μL of reaction mixture from each well was carefully spotted onto the corresponding rectangle on the paper and allowed to dry. The paper was washed with agitation (4 × 5 min in 2× SSC) at room temperature, washed twice with EtOH (5 min), and dried. Rectangles were cut out and placed into scintillation files, 3 mL of scintillation fluid was added to each tube and counts were made for 1 min on a β counter (LKB Rackbeta), counting was controlled by a computer program GENTERM which averaged the mean of the control reaction cocktail blanks and subtracted this background from the test specimen counts. Corrected results were given as counts/minute and a factor of 600 was used to adjust results to cpm/mL. Based on sigmoidal plots of RT activity (cpm) versus inhibitor concentration, the IC_{50} values were determined for each compound.

Anti-HIV activity of 1 and 2 in acutely infected MT2 or PBMC lymphocytes: In these Melbourne studies the degree of inhibition of HIV-1 and HIV-2 by **1** and **2** in acutely infected MT2 cells or PBMCs was determined by measuring the extent by which they reduced HIV-specific cytopathic effects (CPE) at noncytotoxic concentrations. This inhibition was confirmed by measurement of virion-associated reverse transcriptase (RT) activity in cell supernatants. All tests were performed in 48-well tissue culture plates (Costar). Each drug concentration and all controls were tested in duplicate. Virus inoculum was added immediately after the addition of the drugs to the cells.

MT2 cells or PBMCs were counted and resuspended at a concentration of 5 × 10^4/0.25 mL of RF10 medium for MT2-based assays or 3.75 × 10^5/0.25 mL of RF10/IL-2 medium for PBMC-based assays. Compounds **1** and **2** dilutions at twice the final concentration required in the test were prepared in the appropriate medium from a 20 mM stock of the drugs prepared in 60% v/v ethanol. 0.5 mL of each dilution was pipetted into duplicate test and cytotoxicity control wells, followed by the addition of 0.25 mL of cell suspension to all wells. 0.5 mL of RF10 or RF10/IL-2 medium was added to the virus-only controls, 0.75 mL to the cell-only controls and 0.25 mL to the cytotoxicity controls. A volume of 0.25 mL of strain #237288 or HIV-2_{ROD} diluted in the appropriate medium to contain 200 $TCID_{50}$ (for MT2 assays) or 300 $TCID_{50}$ (PBMC assays) was then immediately added to virus-only control wells and the test wells. The plates were then incubated at 37 °C in 5% CO_2. All wells in the test were examined by light microscopy and harvested after 6−7 days incubation, at which time viable cell numbers were determined in cell-only and cytotoxicity control wells using trypan blue dye exclusion counting. Drug dilutions producing cell counts that were less than 90% of the cell-only control were considered to have some degree of toxicity and excluded from calculation of the selective index (SI) of the drug (see below).

The cell-only, virus-only and test cultures were harvested by removing 0.8 mL of supernatant from each well to separate microtubes. The virus present in each supernate was then precipitated using poly(ethylene glycol) and assayed for virion-associated RT activity expressed as counts/minute (cpm) on a liquid scintillation counter as previously described.[29] The percentage (%) inhibition associated with **1** and **2** was calculated by expressing the RT activity at each dilution as a % of the cpm in virus-only controls. The % inhibition was this value subtracted from 100. The SI, which was used as a measure of the relative antiviral activity of **1** and **2**, was calculated using the formula SI = highest noncytotoxic drug concentration (CC_{10}) divided by the lowest inhibitory concentration (the IC_{90}, defined as the drug concentration producing 90% inhibition of virion-associated RT activity in drug-treated, infected cells relative to infected, untreated cells).

Anti-HIV activity of 1 and 2 in lymphocytes chronically infected with HIV-1: In these Melbourne studies H9/HTLV-IIIB cells were incubated in the presence of either 10 μM **1** or **2** or in the absence of drug at 37 °C for 72 h. Supernatant fluid was then removed, clarified at 700*g* for 10 min and virions pelleted by ultracentrifugation at 160000*g* for 1 h at 4 °C in an SW41 rotor using a Beckman L8 ultracentrifuge. Virus pellets were resuspended in saline, then 5× Laemmli sample buffer[30] was added and the samples were stored at −70 °C. For immunoblotting, samples were electro-

phoresed through 10% polyacrylamide gels and transferred to nitrocellulose. After blocking with 3% casein in TBST (50 mM Tris-HCl, pH 7.5, 50 mM NaCl, 0.5% v/v Tween 20) overnight at 4 °C, the blot was stained with a 1 in 1000 dilution of monoclonal antibodies specific for HIV $Pr55^{gag}$ and p24 (reagent ADP313, kindly supplied by Drs. Ferns and Tedder, British Medical Research Council AIDS Reagent Project) for 2 h at room temperature, washed four times with TBST, then incubated for 1 h at room temperature with a 1 in 2000 dilution of anti-mouse IgG conjugated to horseradish peroxidase. Protein bands were detected by chemiluminescence (ECL Western Blot Analysis System, Amersham).

5. Crystallography. Inhibitors **1** and **2** were cocrystallized with synthetic HIV PR. The enzyme was mutated for ease of synthesis and preparation[22] (mutations Q7K, L33I, C37Aba, and C95Aba, where Aba = α-aminobutyric acid). Crystallization was by the hanging drop-vapor diffusion method. The protein was concentrated to 5 mg/mL and a solution of the inhibitor in DMSO was diluted into the protein sample to give an inhibitor:protein molar ratio of 10:1. Protein−inhibitor mixtures were incubated at 4 °C for 24 h prior to crystallization. Reservoir conditions were 0.1 M acetate buffer (pH 5.5) and 35−60% saturated ammonium sulfate. 2−5-μL drops were incubated at 20 °C. Rod shaped crystals appeared within a week and grew over 2−6 weeks.

Data collection and data processing: Crystallographic data were measured at 16 °C using an R-AXIS IIC imaging plate system with Cu Kα X-radiation generated from a Rigaku RU-200 rotating anode generator. Data collection parameters were similar to those described previously.[22] Diffraction data were integrated and scaled using DENZO and SCALEPACK.[31] Statistics from data processing are given in Table 1.

Structure refinement: The two crystal structures were solved by difference Fourier analysis. The starting model was the HIV-1 PR structure from an isomorphous inhibitor complex (PDB code: 1cpi)[15,22] with the inhibitor and solvent molecules removed. X-PLOR 3.851[32] was used for refinement. Cross-validation was performed using *R*-free from 10% of the reflections.[33] Simulated annealing molecular dynamics was performed (temperature = 3000 K), to decouple *R* and *R*-free. Both positional and individual *B*-factor refinements were carried out for several rounds. Protein modeling and rebuilding was performed using O.[34] Parameters for protein refinement were those of Engh and Huber.[35] Water molecules were added where peaks were found in both $|F_o| - |F_c|$ (3σ) and $2|F_o| - |F_c|$ (1σ) maps and where at least one stereochemically reasonable hydrogen bond could be formed. Parameters for the inhibitors were based on equivalent features of peptides modified accordingly, e.g. parameters for the indanyl moiety, **2**, were based on the ring structure of tryptophan. A low resolution cutoff of 8.0 Å and structure factor amplitude cutoff of 0 σF were used during refinement. Refinement statistics are given in Table 2.

In a number of cases where there is poor density for protein side chains, residues have been modeled as alanine or with half-occupancy for side chain atoms. A further group of protein residues have been modeled with two alternative conformations. The majority of these residues are on the surface of the protein. In addition the enzyme main chain atoms of residues Ile150 and Gly150 (located in the flap region above the active site) have been modeled with two alternate conformations. Parts of both inhibitors have also been modeled with either half-occupancy or two conformations including the isosteric hydroxyl of compound **2**.

The programs PROCHECK,[36] WHATCHECK[37] and InsightII 97.0 (MSI) were used. Figure 2 was generated using SETOR.[38] Atomic coordinates and structure factors have been deposited in the Protein Data Bank[39] and HIV data bank[41] (accession codes: 1d4l (**1**), 1d4k (**2**)).

Acknowledgment. We gratefully acknowledge partial financial support from the National Health and Medical Research Council of Australia and the Australian Research Council. J.L.M. is an ARC Senior Research Fellow.

References

(1) Wlodawer, A.; Erickson, J. W. Structure-based inhibitors of HIV-1 protease. *Annu. Rev. Biochem*. **1993**, *62*, 543−85.
(2) Darke, P. L.; Huff, J. R. HIV protease as an inhibitor target for the treatment of AIDS. *Adv. Pharmacol*. **1994**, *25*, 399−454.
(3) West, M. L.; Fairlie, D. P. Targeting HIV-1 protease: a test of drug-design methodologies. *Trends Pharmacol. Sci*. **1995**, *16*, 67−75.
(4) Kempf, D. J.; Sham, H. L. HIV protease inhibitors. *Curr. Pharm. Des*. **1996**, *2*, 225−46.
(5) March, D. R.; Fairlie, D. P. *Designing new antiviral drugs for AIDS: HIV-1 Protease and its inhibitors*; Wise, R., Ed.; R. G. Landes Co.: Austin, TX, 1996.
(6) Wlodawer, A.; Vondrasek, J. Inhibitors of HIV-1 protease: a major success of structure-assisted drug design. *Annu. Rev. Biophys. Biomol. Struct*. **1998**, *27*, 249−84.
(7) Misson, J.; Clark, W.; Kendall, M. J. Therapeutic advances: protease inhibitors for the treatment of HIV-1 infection. *J. Clin. Pharm. Ther*. **1997**, *22*, 109−17.
(8) Hahn, B. H. Viral genes and their products. In *Textbook of AIDS Medicine*; Broder, S., Merigan, T. C., Bolognesi, D., Eds.; Williams and Wilkins: Baltimore, MD, 1994; pp 21−43.
(9) Mildner, A. M.; Rothrock, D. J.; Leone, J. W.; Bannow, C. A.; Lull, J. M.; Reardon, I. M.; Sarcich, J. L.; Howe, W. J.; Tomich, C. S.; Smith, C. W.; et al. The HIV-1 protease as enzyme and substrate: mutagenesis of autolysis sites and generation of a stable mutant with retained kinetic properties. *Biochemistry* **1994**, *33*, 9405−13.
(10) Bukrinsky, M.; Haggerty, S.; Dempsey, M. P.; Sharova, N.; Adhubei, A.; Spitz, P.; Goldfarb, D.; Emerman, M.; Stevenson, M. A nuclear localization signal within HIV-1 matrix protein that governs infection of nondividing cells. *J. Virol*. **1993**, *67*, 6387−94.
(11) Palella, F.; Delaney, K. M.; Moorman, A. C.; Loveless, M. O.; Fuhrer, J.; Satten, G. A.; Aschman, D. J.; Holmberg, S. D. Declining morbidity and mortality among patients with advanced human immunodeficiency virus infection. *N. Engl. J. Med*. **1998**, *338*, 853−60.
(12) Hammer, S. M.; Squires, K. E.; Hughes, M. D.; Grimes, J. M.; Demeter, L. M.; Currier, J. S.; Eron, J. J.; Feinberg, J. E.; Balfour, H. H.; Deyton, L. R.; Chodakewitz, J. A.; Fischl, M. A. A controlled trial of two nucleoside analogues plus indinavir in persons with human immunodeficiency virus infection and CD4 cell counts of 200 per cubic millimeter or less. *N. Engl. J. Med*. **1997**, *337*, 725−33.
(13) Condra, J.; Schlief, W.; Blahy, O.; Gabryelski, L.; Graham, D.; Quintero, J.; Rhodes, A.; Robbins, H.; Roth, E.; Shivaprakash, M.; Titus, E.; Yang, T.; Teppler, H.; Squires, K.; Deutsch, P.; Emini, E. In vivo emergence of HIV-1 variants resistant to multiple protease inhibitors. *Nature* **1995**, *375*, 569−71.
(14) Palmer, S.; Schafer, R. W.; Merigan, T. C. Highly drug-resistant HIV-1 clinical isolates are cross-resistant to many antiretroviral compounds in current clinical development. *AIDS* **1999**, *13*, 661−7.
(15) Abbenante, G.; March, D.; Bergman, D.; Hunt, P. A.; Garnham, B.; Dancer, R. J.; Martin, J. L.; Fairlie, D. P. Regioselective Structural and Functional Mimicry Of Peptides: Design Of Hydrolytically Stable Cyclic Peptidomimetic Inhibitors Of Hiv 1 Protease. *J. Am. Chem. Soc*. **1995**, *117*, 10220−6.
(16) March, D.; Abbenante, G.; Bergman, D.; Brinkworth, R. I.; Wickramasinghe, W.; Begun, J.; Martin, J. L.; Fairlie, D. P. Substrate Based Cyclic Peptidomimetics Of Phe Ile Val That Inhibit Hiv 1 Protease Using a Novel Enzyme Binding Mode. *J. Am. Chem. Soc*. **1996**, *118*, 3375−9.
(17) Reid, R. C.; March, D. R.; Dooley, M. J.; Bergman, D. A.; Abbenante, G.; Fairlie, D. P. A novel bicyclic enzyme inhibitor as a consensus peptidomimetic for the receptor-bound conformations of 12 peptidic inhibitors of HIV-1 protease. *J. Am. Chem. Soc*. **1996**, *118*, 8511−7.
(18) Kim, E. E.; Baker, C. T.; Dwyer, M. D.; Murcko, M. A.; Rao, B. G.; Tung, R. D.; Navia, M. A. Crystal Structure of HIV-1 protease in complex with VX-478, a Potent and Orally Bioavailable Inhibitor of the enzyme *J. Am. Chem. Soc*. **1995**, *117*, 1181−2.
(19) Chen, Z.; Li, Y.; Chen, E.; Hall, D. L.; Darke, P. L.; Culberson, C.; Shafer, J. A.; Kuo, L. C. Crystal structure at 1.9-A resolution of human immunodeficiency virus (HIV) II protease complexed with L-735,524, an orally bioavailable inhibitor of the HIV proteases. *J. Biol. Chem*. **1994**, *269*, 26344−8.
(20) Krohn, A.; Redshaw, S.; Ritchie, J. C.; Graves, B. J.; Hatada, M. H. Novel binding mode of highly potent HIV-proteinase inhibitors incorporating the (R)-hydroxyethylamine isostere. *J. Med. Chem*. **1991**, *34*, 3340−2.

(21) Reid, R. C.; Scanlon, M. J.; Kelso, M. J.; Fairlie, D. P. Synthesis of Conformationally Restrained Cyclic Mimetics Of HIV-1 Protease Substrates. Templates for Combinatorial Development of Protease Inhibitors. *J. Org. Chem*. **2000**, submitted for publication.
(22) Martin, J. L.; Begun, J.; Schindeler, A.; Wickramasinghe, W. A.; Alewood, D.; Alewood, P. F.; Bergman, D. A.; Brinkworth, R. I.; Abbenante, G.; March, D.; Reid, R. C.; Hunt, P. A.; Fairlie, D. P. Molecular Recognition of Macrocyclic Peptidomimetic inhibitors by HIV-1 Protease. *Biochemistry* **1999**, *38*, 7978−88.
(23) Rose, J. R.; Salto, R.; Craik, C. S. Regulation of autoproteolysis of the HIV-1 and HIV-2 proteases with engineered amino acid substitutions. *J. Biol. Chem*. **1993**, *268*, 11939−45.
(24) Swain, A. L.; Miller, M. M.; Green, J.; Rich, D. H.; Schneider, J.; Kent, S. B.; Wlodawer, A. X-ray crystallographic structure of a complex between a synthetic protease of human immunodeficiency virus 1 and a substrate-based hydroxyethylamine inhibitor. *Proc. Natl. Acad. Sci. U.S.A.* **1990**, *87*, 8805−9.
(25) Tyndall, J. D. A.; Fairlie, D. P. Conformational Homogeneity in Molecular Recognition by Proteolytic Enzymes. *J. Mol. Recognit.* **1999**, *12*, 1−8.
(26) Schneider, J.; Kent, S. B. Enzymatic activity of a synthetic 99 residue protein corresponding to the putative HIV-1 protease. *Cell* **1988**, *54*, 363−8.
(27) Bergman, D. A.; Alewood, D.; Alewood, P. F.; Andrews, J. L.; Brinkworth, R. I.; Englebretsen, D. R.; Kent, S. B. H. Kinetic-properties of HIV-1 Protease Produced by Total Chemical Synthesis with Cysteine Residues Replaced by Isosteric L-alpha-amino-*n*-butyric Acid. *Lett. Pept. Sci.* **1995**, *2*, 99−107.
(28) Tachedjian, G.; Tyssen, D.; Locarnini, S.; Gust, I.; Birch, C. Investigation of topoisomerase inhibitors for activity against human immunodeficiency virus: inhibition by coumermycin A1. *Antivir. Chem. Chemother.* **1990**, *1*, 131−8.
(29) Neate, E. V.; Pringle, R. C.; Jowett, J. B. M.; Healey, D. S.; Gust, I. D. Isolation of HIV from Australian patients with AIDS, AIDS-related conditions and healthy antibody positive individuals. *Aust. New Zealand J. Med.* **1987**, *17*, 461−6.
(30) Laemmli, U. K. Cleavage of structural proteins during the assembly of the head of bacteriophage T4. *Nature* **1970**, *227*, 680−5.
(31) Otwinski, Z.; Minor, W. Processing of X-ray diffraction data collected in oscillation mode. *Methods Enzymol.* **1997**, *276*, 307−26.
(32) Brünger, A. T. *X-PLOR (Version 3.1) Manual*; Yale University: New Haven, CT, 1992.
(33) Brünger, A. T. Assessment of phase accuracy by cross validation: the free *R* value. Methods and applications. *Acta Crystallogr. D* **1993**, *D46*, 24−36.
(34) Jones, T. A.; Zou, J. Y.; Cowan, S. W.; Kjeldgaard, M. Improved methods for building protein models in electron density maps and the location of errors in these models. *Acta Crystallogr. A* **1991**, *47*, 110−9.
(35) Engh, R. A.; Huber, R. Accurate bond and angle parameters for X-ray protein structure refinement. *Acta Crystallogr*. **1991**, *A47*, 392−400.
(36) Laskowski, R. A.; MacArthur, M. W.; Moss, D. S.; Thornton, J. M. PROCHECK: A program to check the stereochemical quality of protein structures. *J. Appl. Crystallogr.* **1993**, *26*, 283−91.
(37) Hooft, R. W. W.; Vriend, G.; Sander, C.; Abola., E. E. WHAT_CHECK (verification routines from WHAT IF). Errors in protein structures. *Nature* **1996**, *381*, 272.
(38) Evans, S. V. SETOR: hardware-lighted three-dimensional solid model representations of macromolecules. *J. Mol. Graph*. **1993**, *11*, 134−8, 127−8.
(39) Berman, H. M.; Westbrook, J.; Feng, Z.; Gilliand, G.; Bhat, T. N.; Weissig, H.; Shindyalov, I. N.; Bourne, P. E. The Protein Data Bank. *Nucleic Acids Res.* **2000**, *28*, 235−242.
(40) Fairlie, D. P.; Tyndall, J. D. A.; Reid, R. C.; Wong, A. K.; Abbenante, G.; Scanlon, M. J.; March, D. R.; Bergman, D. A.; Chai, C. L. L.; Burkett, B. A. Conformational Selection of Inhibitors and Substrates by Proteolytic Enzymes: Implications for Drug Design and Polypeptide Processing. *J. Med. Chem*. **2000**, *43*, 1271−1281.
(41) Vondrasek, J.; van Buskirk, C. P.; Wlodawer, A. Database of three-dimensional structures of HIV proteinases *Nat. Struct. Biol*. **1997**, *4*, 8.
(42) Luzzati, V. Traitment statistique des erreurs dans la determination des structures cristallines. *Acta Crystallogr*. **1952**, *5*, 802−810.

JM000013N